

High-order-harmonic generation by Laguerre-Gaussian laser modes: Control of the spectra by manipulating the spatial medium distribution

Dmitry A. Telnov^{1,*} and Shih-I Chu^{2,3,†}¹*Department of Physics, St. Petersburg State University, 7-9 Universitetskaya Naberezhnaya, St. Petersburg 199034, Russia*²*Center for Quantum Science and Engineering, Department of Physics, National Taiwan University, Taipei 10617, Taiwan*³*Department of Chemistry, University of Kansas, Lawrence, Kansas 66045, USA*

(Received 3 August 2017; published 6 September 2017)

We study high-order-harmonic generation (HHG) by the incident laser beam in the Laguerre-Gaussian mode with a nonzero topological charge. We find that the harmonic signal in the central spot on the beam axis does not always vanish and depends on the distribution of the medium in the focal region of the incident laser beam. The HHG spectra on the beam axis can be controlled by changing the spatial medium distribution. General theoretical results are confirmed by calculations of HHG in the medium of argon atoms, with the single-atom response obtained by means of the time-dependent density functional theory.

DOI: [10.1103/PhysRevA.96.033807](https://doi.org/10.1103/PhysRevA.96.033807)

I. INTRODUCTION

Laser beams carrying orbital angular momentum (OAM) [1] and their interaction with matter are currently of much interest in both theory and experiment because of their unique properties. Such beams are also termed optical vortices since the local momentum distribution mimics the velocity pattern of a tornado or a vortex fluid. Another name for the same photon state is twisted light beam (or twisted photons) because of the waterfront spiraling about the propagation direction of the beam [2]. In the infrared and visible spectral regions, optical vortices are readily produced using spiral phase plates [3,4], computer-generated holograms [5,6], or combinations of astigmatic optical elements [7]. Numerous applications of twisted light beams are available or anticipated in the near future in various areas such as quantum information and communication [8,9], imaging and microscopy [10,11], nanoparticles and nanostructures control and manipulation [12–14], and others.

A widely used example of the electromagnetic radiation with OAM is the Laguerre-Gaussian (LG) laser mode. This mode is a solution of the wave equation in the paraxial regime where the wave propagation is limited to directions within a small angle of the beam axis. It should be noted that disentanglement of the photon spin and the OAM is possible in the paraxial approximation only. In the general case, the total angular momentum must be considered (see, for example, Ref. [15], where different solutions of the wave equation [Bessel beams] valid beyond the paraxial approximation are studied). For the monochromatic linearly polarized LG wave propagating along the z axis, the electric field strength \mathcal{E} can be expressed as follows:

$$\mathcal{E}(r, \varphi, z, t) = \mathcal{E}_0 \hat{x} \text{Re}\{u(r, \varphi, z) \exp[-i(kz - \omega t)]\}, \quad (1)$$

where \mathcal{E}_0 is the electric field amplitude, \hat{x} is a unit vector along the polarization direction (x axis), ω is the frequency, and $k = \omega/c$ is the wave number (c being the speed of light). Cylindrical coordinates r , φ , and z are used in Eq. (1) with r

being the distance from the z axis in the transverse plane x - y , φ being the azimuthal angle about the z axis, and z being the distance in the propagation direction. The function $u(r, \varphi, z)$ has an analytic form:

$$u = \frac{w_0}{w(z)} \left(\frac{r\sqrt{2}}{w(z)} \right)^{|l|} \exp(-il\varphi) L_p^{|l|} \left(\frac{2r^2}{[w(z)]^2} \right) \times \exp\left(-\frac{r^2}{[w(z)]^2}\right) \exp\left(-i\frac{kr^2}{2R(z)}\right) \exp[i\psi(z)], \quad (2)$$

where the notation $L_p^{|l|}$ stands for the generalized Laguerre polynomial. Integer numbers l and p define the mode; l is called the topological charge (in the photon picture, it is equal to the projection of the orbital angular momentum of the photon onto its momentum). In Eq. (2), w_0 is the waist radius of the beam; the beam width $w(z)$ depends on the distance along the z axis:

$$w(z) = w_0 \sqrt{1 + \left(\frac{z}{z_R} \right)^2}, \quad (3)$$

where

$$z_R = \frac{\pi w_0^2}{\lambda} \quad (4)$$

is called the Rayleigh range (λ being the wavelength). Other quantities in Eq. (2) are the radius of the curvature of the wave front $R(z)$,

$$R(z) = z \left[1 + \left(\frac{z_R}{z} \right)^2 \right], \quad (5)$$

and the Gouy phase $\psi(z)$,

$$\psi(z) = (|l| + 2p + 1) \arctan\left(\frac{z}{z_R}\right). \quad (6)$$

The signatures of the LG mode with a nonzero topological charge are the dependence of the phase on the azimuthal angle φ and a donut-shaped intensity profile in the transverse x - y plane with the dark spot in the vicinity of the beam axis.

Generation of twisted beams in the extreme-ultraviolet (XUV) spectral range and their interaction with atoms and molecules have recently attracted increasing attention. It

*d.telnov@spbu.ru

†sichu@ku.edu

was shown theoretically that OAM could be transferred to the electronic degrees of freedom [15–17] and induce charge current loops in fullerenes with an associated orbital magnetic moment [18]. Intense XUV beams carrying OAM can be possibly produced by free-electron lasers; the technical schemes have been proposed [19,20]. High-order-harmonic generation (HHG) is a tabletop alternative to free-electron lasers, where optical vortices originally generated in the near-infrared wavelength range can be converted to the XUV range by means of a nonlinear interaction with matter. Several experimental observations of twisted high-order harmonics in gases have been reported [21–24]. While the first experiment [21] detected all the harmonics with the topological charge 1 (equal to that of the incident LG beam), subsequent studies [22,23] showed that the topological charge is a multiple of the harmonic order, in accordance with the theoretical considerations about angular momentum conservation [25]. In Ref. [23], experimental synthesis of attosecond XUV “light springs” (ultrashort spatiotemporal light pulses where both the phase and the intensity profiles have helical structures [26]) was reported. Very recently, an experimental scheme has been proposed that allows generation of harmonics carrying arbitrary topological charge for any harmonic order [24].

In this communication, we report on a specific aspect of HHG by LG beams, power spectra of the harmonics propagating in the central spot of the beam. For the incident LG mode, this spot is dark, and the intensity totally vanishes on the beam axis. Normally, the same property is preserved for the generated harmonics. However, as we show, harmonic radiation still can be observed in the central spot, depending on the distribution of the medium atoms in the focal region of the incident beam. Manipulating this distribution, one can control the shape of the HHG spectra, switching on and off regions with the specific harmonic orders.

II. THEORETICAL DESCRIPTION

Since HHG is a highly nonlinear process, the harmonic radiation power has a sharp dependence on the intensity of the incident laser field. That is why it would be a reasonable approximation if we restricted our treatment to the spatial region where the electric field (or intensity) of the incident beam reaches its maximum. For the LG laser mode with $p = 0$, this is a circle in the transverse plane $z = 0$ with the radius $r_0 = w_0\sqrt{l/2}$ [see Eq. (2)]. The beam waist w_0 measured in the experiments is about $40 \mu\text{m}$ [21,23] for the driving field wavelength of 800 nm. That means the radius of the circle with the peak intensity is much larger than the laser wavelength and by far exceeds the atomic size. Therefore individual atoms distributed along this circle may not “see” the global geometric structure of the LG mode (both intensity and phase), and their interaction with the “local” field (in the vicinity of each atom) can be described within the traditional dipole approximation. Then each atom would generate usual harmonics with plane wave fronts. Generation of LG harmonics is thus a collective coherent response of a large number of medium atoms in the interaction region.

For the monochromatic driving field of frequency ω_0 , the spatial and temporal dependence of the electric field on the

circle with the peak intensity can be expressed as follows:

$$\mathcal{E}(\varphi, t) = \mathcal{E}_0 \sin(\omega_0 t - l\varphi). \quad (7)$$

For the pulsed field, a temporal envelope must be also included in Eq. (7). Each atom on the circle (or group of atoms since we are talking about the distribution on the circle of a macroscopic radius) can be assigned a specific value of the azimuthal angle φ . The electric field at an arbitrary φ position is phase-shifted with respect to the field at $\varphi = 0$. According to Eq. (7), the same phase shift can be achieved by an appropriate time delay, and the following relation holds:

$$\mathcal{E}(\varphi, t) = \mathcal{E}(0, t - l\varphi/\omega_0). \quad (8)$$

We note that Eq. (8) is exact for the monochromatic field only and can be regarded as an approximation for the pulsed field with the temporal envelope. According to the widely used semiclassical theory of HHG, the electric vector of the emitted radiation is proportional to the induced dipole acceleration $\mathbf{a}(t)$ [27], and the latter is calculated as an expectation value of the corresponding quantum operator:

$$\mathbf{a}(t) = -\langle \Psi(t) | \nabla V(t) | \Psi(t) \rangle, \quad (9)$$

where $\Psi(t)$ is the wave function of the atom in the external field and $V(t)$ is the total time-dependent potential. For the atom with the coordinate φ on the circle, the wave function $\Psi(t)$ is a solution of the time-dependent Schrödinger equation with the external field given by Eq. (8). That is why the dipole acceleration $\mathbf{a}(\varphi, t)$ of the atom calculated according to Eq. (9) satisfies the relation similar to that in Eq. (8):

$$\mathbf{a}(\varphi, t) = \mathbf{a}(0, t - l\varphi/\omega_0). \quad (10)$$

Performing the Fourier transformation of Eq. (10), one immediately obtains

$$\tilde{\mathbf{a}}(\varphi, \omega) = \exp\left(i\frac{l\varphi\omega}{\omega_0}\right)\tilde{\mathbf{a}}(0, \omega). \quad (11)$$

Once the harmonic radiation is emitted, the wave equation must be solved to propagate it through the medium to the far-field region. The propagation may insert additional phase differences between the contributions of different atoms to the total signal at the position of the observer. However, if the detector is placed in the central spot on the beam axis, such phase differences do not arise, and the total harmonic signal can be calculated with the total dipole acceleration, which is a coherent sum of the dipole accelerations of individual groups of atoms:

$$\tilde{\mathbf{a}}_{\text{tot}}(\omega) = \tilde{\mathbf{a}}(0, \omega) \int_0^{2\pi} d\varphi \rho(\varphi) \exp\left(i\frac{l\varphi\omega}{\omega_0}\right). \quad (12)$$

Here $\rho(\varphi)$ is the distribution density function for the atoms on the circle. One can easily see from Eq. (12) that for the uniform distribution [$\rho(\varphi) = \rho_0$] the total dipole acceleration in the central spot vanishes for any nonzero topological charge l and integer harmonic order ω/ω_0 , as it should be the case for the LG mode. However, for specially crafted and nonuniform distributions, the harmonic radiation can still be detected in the central spot. Below we consider the cases of discrete and continuous distributions.

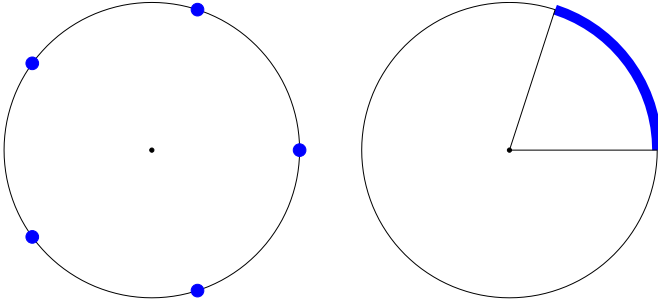


FIG. 1. Discrete (left panel) and continuous (right panel) medium distribution on the circle in the transverse plane of the laser beam.

A. Discrete medium distribution

Suppose we have N groups of atoms uniformly distributed on the circle where the laser field strength reaches its maximum (Fig. 1, left panel). For the LG beam with the topological charge l , the phase difference of the field between two adjacent groups is equal to $2\pi l/N$. Then the Fourier transform of the dipole acceleration of the j th group reads as

$$\tilde{\mathbf{a}}_j(\omega) = \exp\left[i\frac{2\pi lj}{N\omega_0}\right]\tilde{\mathbf{a}}_0(\omega). \quad (13)$$

To calculate the total dipole acceleration, we replace integration over φ in Eq. (12) with summation:

$$\begin{aligned} \tilde{\mathbf{a}}_{\text{tot}}(\omega) &= \tilde{\mathbf{a}}_0(\omega) \sum_{j=0}^{N-1} \exp\left[i\frac{2\pi lj}{N\omega_0}\right] \\ &= \tilde{\mathbf{a}}_0(\omega) \exp\left[i\frac{\pi l\omega(N-1)}{\omega_0 N}\right] \frac{\sin\left(\frac{\pi l\omega}{\omega_0}\right)}{\sin\left(\frac{\pi l\omega}{N\omega_0}\right)}. \end{aligned} \quad (14)$$

The power of harmonic radiation $P(\omega)$ is proportional to the squared absolute value of the Fourier-transformed dipole acceleration. Then we obtain that the total and single-group power spectra are related to each other by a simple profile function:

$$P_{\text{tot}}(\omega) = f_{l,N}(\omega)P_0(\omega), \quad (15)$$

$$f_{l,N}(\omega) = \frac{\sin^2\left(\frac{\pi l\omega}{\omega_0}\right)}{\sin^2\left(\frac{\pi l\omega}{N\omega_0}\right)}. \quad (16)$$

The numerator in Eq. (16) vanishes at any integer ω/ω_0 . Since the harmonic order (ratio ω/ω_0) must be an odd integer number (for the atoms or molecules with inversion symmetry), the whole function $f_{l,N}(\omega)$ may vanish at some harmonic orders $2n+1$, depending on the behavior of the denominator. The general rule is as follows: if $l(2n+1)/N$ is *not* an integer number, then generation of the $(2n+1)$ th harmonic is suppressed. Otherwise the power of this harmonic is increased by the factor N^2 compared with the harmonic power of a single group of atoms. Consequently, if l is *odd* and N is *even*, then HHG is totally suppressed. Symmetric distribution with an even number of groups on the circle does not generate harmonics in the central spot when driven by the LG beam with the odd topological charge. If both l and N are odd, and N/l is *not* integer, only harmonics with the orders $(2n+1)N$ are generated.

TABLE I. Nonvanishing harmonic orders in the central spot for the topological charges 1 to 3 and discrete symmetric distribution on the circle with the number of groups 2 to 6.

l	N	Nonvanishing harmonics
1	2	None
1	3	3, 9, 15, 21, 27, 33, ...
1	4	None
1	5	5, 15, 25, 35, 45, 55, ...
2	2	All
2	3	3, 9, 15, 21, 27, 33, ...
2	4	None
2	5	3, 9, 15, 21, 27, 33, ...
2	6	5, 15, 25, 35, 45, 55, ...
3	2	None
3	3	All
3	4	None
3	5	5, 15, 25, 35, 45, 55, ...

If both l and N are odd, and $N/l = M$ is another odd integer, only harmonics with the orders $(2n+1)M$ are generated.

Consider the lowest nonzero topological charge $l=1$. For the symmetric distribution on the circle, HHG in the central spot is possible if N is odd. In this case, harmonics with the orders $(2n+1)N$ are generated; spacing between two adjacent nonvanishing harmonic peaks is equal to $2N$. For $l=2$, HHG on the beam axis is suppressed if both N and $N/2$ are even. Otherwise, HHG is possible in two different cases. If N is even and $N/2$ is odd, harmonics with the orders $(2n+1)N/2$ are generated; spacing between two adjacent nonvanishing harmonic peaks is equal to N . If N is odd, harmonics with the orders $(2n+1)N$ are generated; spacing between two adjacent nonvanishing harmonic peaks is equal to $2N$. The general rules are illustrated in Table I for the topological charges 1 to 3 and number of groups 2 to 6.

B. Continuous medium distribution

For the continuous uniform medium distribution on the circle, one can either use Eq. (12) with the constant distribution function $\rho(\varphi) = \rho_0$ or take a limit $N \rightarrow \infty$ in Eq. (16). In the latter case, the following relation between the total and single-group power spectra is obtained:

$$P_{\text{tot}}(\omega) = N^2 f_l(\omega)P_0(\omega), \quad (17)$$

$$f_l(\omega) = \left(\frac{\omega_0}{\pi l\omega}\right)^2 \sin^2\left(\frac{\pi l\omega}{\omega_0}\right). \quad (18)$$

As one can see, the function $f_l(\omega)$ turns zero at all integer harmonic orders ω/ω_0 unless $l=0$. As it was stated above, uniformly and continuously distributed medium on the whole circle does not generate harmonics in the central spot under the LG laser field with a nonzero topological charge. Harmonic generation is possible, however, if the axial symmetry of the distribution is somehow broken. For example, HHG in the central spot does exist if the medium fills not the whole circle but only an arc corresponding to the central angle $2\pi\beta$ ($0 < \beta < 1$, see Fig. 1, right panel). In the latter case, the profile

function $f_{l,\beta}(\omega)$ in Eq. (17) is calculated as

$$f_{l,\beta}(\omega) = \left(\frac{\omega_0}{\pi l \beta \omega} \right)^2 \sin^2 \left(\frac{\pi l \beta \omega}{\omega_0} \right). \quad (19)$$

Depending on the β value, it does not turn zero at every harmonic order. The HHG spectrum, however, has a frequency-dependent attenuation, compared with the single-group response. When the frequency ω is increasing, the harmonic signal is decreasing as $1/\omega^2$.

III. HHG SPECTRA OF ARGON

We have performed calculations of HHG in argon atoms subject to the laser pulses in the LG mode with $l = 1$ and $p = 0$. The carrier wavelength of the incident beam is 800 nm. The temporal pulse envelope has a \sin^2 shape with a peak intensity of 2×10^{14} W/cm²; several pulse durations have been used in the calculations. For the laser pulse (rather than continuous wave), we define the spectral density of the radiation energy emitted for the whole pulse duration [27]:

$$S(\omega) = \frac{2}{3\pi c^3} |\tilde{\mathbf{a}}_{\text{tot}}(\omega)|^2, \quad (20)$$

and the total dipole acceleration is a sum of the individual atom contributions:

$$\tilde{\mathbf{a}}_{\text{tot}}(\omega) = \sum_{j=0}^{N-1} \tilde{\mathbf{a}}_j(\omega). \quad (21)$$

We use Eq. (21) instead of Eq. (14) for the monochromatic field. However, as our results show, the approximation (14) appears quite good for long enough laser pulses.

The single-atom responses $\tilde{\mathbf{a}}_j(\omega)$ are obtained within the framework of the time-dependent density functional theory (TDDFT). We use the LB94 [28] exchange-correlation potential which has proper long-range asymptotics and proved quite accurate in the electron structure and time-dependent calculations of Ar atoms [29–31]. The time-dependent Kohn-Sham equations are solved by the generalized pseudospectral (GPS) method in spherical polar coordinates, and the time-dependent GPS split-operator method [32] is used for the time propagation. Exterior complex scaling technique [33,34] is applied to impose the correct boundary conditions on the wave functions and prevent spurious reflections from the boundaries of the spatial box where the problem is solved. In the present calculations, we use 256 radial and 24 angular grid points and 4096 time steps per optical cycle of the driving field. The exterior complex scaling region begins at 25 atomic units (a.u.) from the nucleus, and the total linear dimension of the spatial box is 200 a.u. When calculating the dipole acceleration with the Kohn-Sham orbitals according to Eq. (9), only the nuclear and external field potentials are used for evaluation of the expectation values since the Hartree and exact exchange-correlation potentials do not contribute to the total dipole acceleration (zero-force theorem [35]). A detailed description of our implementation of the TDDFT approach and numerical procedure can be found in Ref. [30].

As an example of discrete medium distribution on the circle, we take three equally spaced argon atoms. The field strengths of the linearly polarized driving laser at each atom position

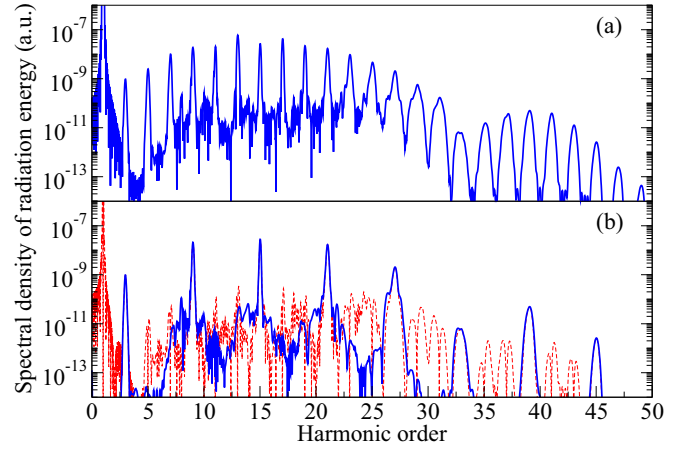


FIG. 2. HHG spectra of Ar atoms by LG laser pulse with the \sin^2 temporal envelope, a carrier wavelength of 800 nm, a peak intensity of 2×10^{14} W/cm², and a total duration of 20 optical cycles. (a) Single-atom spectrum. (b) Normalized spectrum produced by symmetric distribution of three atoms on the circle. The blue solid line shows the results obtained by Eq. (21), and the red dashed line corresponds to the approximation (14).

differ by the carrier-envelope phase:

$$\mathcal{E}(j,t) = \mathcal{E}_0 \sin^2 \frac{\pi t}{T} \sin \left(\omega_0 t - \frac{2\pi l j}{N} \right), \quad j = 0, \dots, N-1, \quad (22)$$

where T is the pulse duration; $l = 1$ and $N = 3$ for this set of the calculations. The single-atom dipole accelerations are computed by solving a system of the time-dependent Kohn-Sham equations for each carrier-envelope phase, and the total response is calculated according to Eq. (21). In Fig. 2, the HHG spectra for the total pulse duration of 20 optical cycle cycles [full width at half maximum (FWHM) is about 27 fs] are presented (for the comparison with the single-atom data on the same scale, here and below all N -atom spectra are divided by N^2). While the single-atom spectrum contains all odd harmonics at full strength (a minimum at the 33rd harmonic is a manifestation of the famous Cooper minimum [36] in HHG, see discussion in Ref. [30] and references therein), the collective three-atom response exhibits well-shaped harmonics of the orders 3, 9, 15, 21, etc. only, in agreement with the theoretical predictions in Table I. Along with the results based on Eq. (21), we also show the spectrum obtained with the help of the approximate equation (14). As one can see, for this long enough laser pulse, performance of the approximation (14) is quite good, especially in the low-energy part of the spectrum where the single-atom harmonics are narrow (note that in the monochromatic field approximation harmonics must be infinitely narrow). In the above-threshold higher-energy region with broad single-atom harmonic peaks, a simple multiplication of the single-atom spectrum by the profile function (16) results in the appearance of spurious peak structures with amplitudes comparable with that of the true harmonics in the three-atom spectrum.

In Fig. 3, the HHG spectra are presented for the same symmetric three-atom distribution on the circle and much shorter laser pulse (4 optical cycles or 5.3 fs FWHM). For

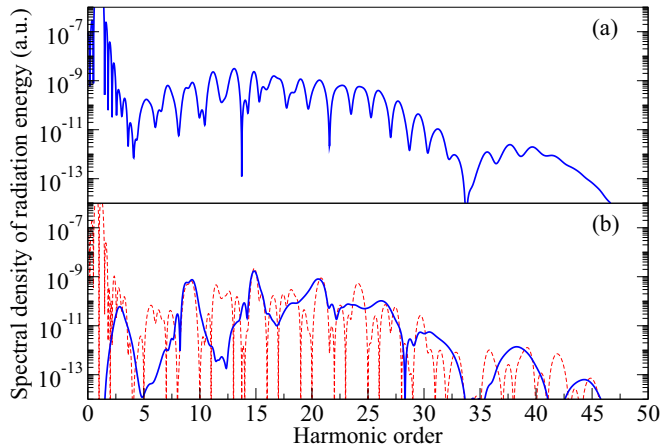


FIG. 3. HHG spectra of Ar atoms by LG laser pulse with the \sin^2 temporal envelope, a carrier wavelength of 800 nm, a peak intensity of 2×10^{14} W/cm², and a total duration of 4 optical cycles. (a) Single-atom spectrum. (b) Normalized spectrum produced by symmetric distribution of three atoms on the circle. The blue solid line shows the results obtained by Eq. (21), and the red dashed line corresponds to the approximation (14).

such a short pulse, the single-atom HHG spectrum has a high background and broad harmonic peaks. In this respect, it is interesting to see that the three-atom spectrum exhibits well-shaped harmonic peaks with the orders 3, 9, and 15 with deep minima between them. This is evidently a result of interference of individual atom contributions to the total harmonic signal, which appears constructive at the peak positions and destructive between them. As expected, the monochromatic field approximation for the HHG spectrum based on Eq. (14) does not work well for this pulse duration. Although the peaks at the harmonic orders 9 and 15 are reproduced accurately, the whole spectrum differs very much from that calculated according to Eq. (21).

To simulate a continuous medium distribution, we apply the same approach as for a discrete distribution but use a large number of atoms uniformly distributed on the arc of the circle. For this set of the calculations, 128 argon atoms occupy one-third of the circle ($\beta = 1/3$), the topological charge $l = 1$, and the pulse duration T is equal to 8 optical cycles (FWHM 10.7 fs). The profile function $f_{l,\beta}(\omega)$ calculated in the monochromatic approximation (19) predicts that for $\beta = 1/3$ harmonics with the orders divisible by 3 must vanish in the central spot of the laser beam. In other words, nonvanishing harmonics have the orders 5, 7, 11, 13, and so on. As one can see from Fig. 4, this is indeed the case. Moreover, the monochromatic approximation for the HHG spectrum appears surprisingly accurate in the case of continuous medium distribution, although the pulse duration is not very long in this calculation. Not only are the heights and widths of the harmonic peaks reproduced correctly but also the attenuation of the spectrum with increasing frequency is reproduced correctly, compared with the fully numerical results based on Eq. (21).

IV. CONCLUSION

In this paper, we have studied HHG in the central spot on the incident laser beam axis when the driving field is in

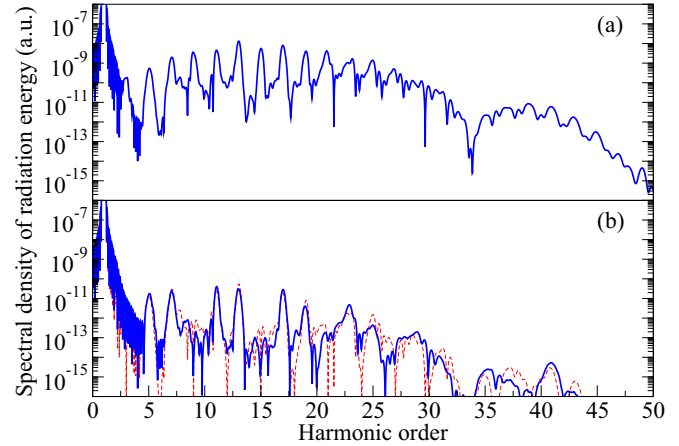


FIG. 4. HHG spectra of Ar atoms by LG laser pulse with the \sin^2 temporal envelope, a carrier wavelength of 800 nm, a peak intensity of 2×10^{14} W/cm², and a total duration of 8 optical cycles. (a) Single-atom spectrum. (b) Normalized spectrum produced by uniform distribution of 128 atoms on one-third of the circle. The blue solid line shows the results obtained by Eq. (21), and the red dashed line corresponds to the monochromatic approximation with the profile function (19).

the LG mode with the nonzero topological charge. It has been experimentally confirmed [21–24] that normally the LG incident beam generates harmonics in the LG modes as well. Consequently, the intensity of the harmonic radiation vanishes on the beam axis. We have shown that this is not always the case, and depending on the medium distribution in the focal region of the driving laser, the harmonic signal can be detected in the central spot on the beam axis. Moreover, by a special preparation of this distribution, it is possible to control the shape of the HHG spectrum, switching on and off harmonics with particular orders or changing their intensity. This additional control of the HHG spectrum could be useful in generation of attosecond pulses. Although a discussion of possible experimental confirmation of our theoretical predictions is beyond the scope of this paper, we can mention here that a simple way to achieve a continuous distribution that does not possess the axial symmetry on the circle in the transverse plane of the laser focus could be using a setup geometry with incomplete overlap between the laser beam and the gas jet. In this case, only a part of the circle corresponding to the maximum intensity of the LG mode would be filled with the medium atoms, thus providing conditions for HHG in the central spot of the laser beam.

ACKNOWLEDGMENTS

This work was partially supported by the Chemical Sciences, Geosciences and Biosciences Division of the Office of Basic Energy Sciences, Office of Sciences, U.S. Department of Energy under Grant No. DE-FG02-04ER15504. We also acknowledge the partial support of the Ministry of Science and Technology of Taiwan and National Taiwan University (Grants No. 106R891701 and No. 106R8700-2). D.A.T. acknowledges the partial support from Russian Foundation for Basic Research (Grant No. 16-02-00233).

- [1] L. Allen, M. W. Beijersbergen, R. J. C. Spreeuw, and J. P. Woerdman, *Phys. Rev. A* **45**, 8185 (1992).
- [2] G. Molina-Terriza, J. P. Torres, and L. Torner, *Nat. Phys.* **3**, 305 (2007).
- [3] S. N. Khonina, V. V. Kotlyar, M. V. Shinkaryev, V. A. Soifer, and G. V. Uspleniev, *J. Mod. Opt.* **39**, 1147 (1992).
- [4] M. W. Beijersbergen, R. P. C. Coerwinkel, M. Kristensen, and J. P. Woerdman, *Opt. Commun.* **112**, 321 (1994).
- [5] V. Y. Bazhenov, M. V. Vasnetsov, and M. S. Soskin, *JETP Lett.* **52**, 429 (1990).
- [6] N. R. Heckenberg, R. McDuff, C. P. Smith, and A. G. White, *Opt. Lett.* **17**, 221 (1992).
- [7] G. Nienhuis and L. Allen, *Phys. Rev. A* **48**, 656 (1993).
- [8] E. Nagali, L. Sansoni, F. Sciarrino, F. De Martini, L. Marrucci, B. Piccirillo, E. Karimi, and E. Santamato, *Nat. Photon.* **3**, 720 (2009).
- [9] J. Wang, J.-Y. Yang, I. M. Fazal, N. Ahmed, Y. Yan, H. Huang, Y. Ren, Y. Yue, S. Dolinar, M. Tur, and A. E. Willner, *Nat. Photon.* **6**, 488 (2012).
- [10] S. Fürhapter, A. Jesacher, S. Bernet, and M. Ritsch-Marte, *Opt. Lett.* **30**, 1953 (2005).
- [11] S. Bernet, A. Jesacher, S. Fürhapter, C. Maurer, and M. Ritsch-Marte, *Opt. Express* **14**, 3792 (2006).
- [12] D. G. Grier, *Nature (London)* **424**, 810 (2003).
- [13] A. M. Yao and M. J. Padgett, *Adv. Opt. Photon.* **3**, 161 (2011).
- [14] K. Toyoda, K. Miyamoto, N. Aoki, R. Morita, and T. Omatsu, *Nano Lett.* **12**, 3645 (2012).
- [15] O. Matula, A. G. Hayrapetyan, V. G. Serbo, A. Surzhykov, and S. Fritzsche, *J. Phys. B* **46**, 205002 (2013).
- [16] A. Picón, J. Mompart, J. R. Vázquez de Aldana, L. Plaja, G. F. Calvo, and L. Roso, *Opt. Express* **18**, 3660 (2010).
- [17] H. M. Scholz-Marggraf, S. Fritzsche, V. G. Serbo, A. Afanasev, and A. Surzhykov, *Phys. Rev. A* **90**, 013425 (2014).
- [18] J. Wätzel, Y. Pavlyukh, A. Schäffer, and J. Berakdar, *Carbon* **99**, 439 (2016).
- [19] E. Hemsing, A. Knyazik, M. Dunning, D. Xiang, A. Marinelli, C. Hast, and J. B. Rosenzweig, *Nat. Phys.* **9**, 549 (2013).
- [20] P. R. Ribič, D. Gauthier, and G. De Ninno, *Phys. Rev. Lett.* **112**, 203602 (2014).
- [21] M. Zürch, C. Kern, P. Hansinger, A. Dreischuh, and C. Spielmann, *Nat. Phys.* **8**, 743 (2012).
- [22] G. Gariépy, J. Leach, K. T. Kim, T. J. Hammond, E. Frumker, R. W. Boyd, and P. B. Corkum, *Phys. Rev. Lett.* **113**, 153901 (2014).
- [23] R. Géneaux, A. Camper, T. Auguste, O. Gobert, J. Caillat, R. Taïeb, and T. Ruchon, *Nat. Commun.* **7**, 12583 (2016).
- [24] D. Gauthier, P. Rebernik Ribič, G. Adhikary, A. Camper, C. Chappuis, R. Cucini, L. F. DiMauro, G. Dovillaire, F. Frassetto, R. Géneaux, P. Miotti, L. Poletto, B. Ressel, C. Spezzani, M. Stupar, T. Ruchon, and G. De Ninno, *Nat. Commun.* **8**, 14971 (2017).
- [25] C. Hernández-García, A. Picón, J. San Román, and L. Plaja, *Phys. Rev. Lett.* **111**, 083602 (2013).
- [26] G. Pariente and F. Quéré, *Opt. Lett.* **40**, 2037 (2015).
- [27] L. D. Landau and E. M. Lifshitz, *The Classical Theory of Fields* (Pergamon Press, Oxford, 1975).
- [28] R. van Leeuwen and E. J. Baerends, *Phys. Rev. A* **49**, 2421 (1994).
- [29] X. Wang, M. Chini, Q. Zhang, K. Zhao, Y. Wu, D. A. Telnov, S.-I. Chu, and Z. Chang, *Phys. Rev. A* **86**, 021802(R) (2012).
- [30] D. A. Telnov, K. E. Sosnova, E. Rozenbaum, and S.-I. Chu, *Phys. Rev. A* **87**, 053406 (2013).
- [31] M. Chini, X. Wang, Y. Cheng, H. Wang, Y. Wu, E. Cunningham, P.-C. Li, J. Heslar, D. A. Telnov, S.-I. Chu, and Z. Chang, *Nat. Photon.* **8**, 437 (2014).
- [32] X.-M. Tong and S.-I. Chu, *Chem. Phys.* **217**, 119 (1997).
- [33] C. A. Nicolaides and D. R. Beck, *Phys. Lett. A* **65**, 11 (1978).
- [34] B. Simon, *Phys. Lett. A* **71**, 211 (1979).
- [35] G. Vignale, *Phys. Rev. Lett.* **74**, 3233 (1995).
- [36] J. W. Cooper, *Phys. Rev.* **128**, 681 (1962).